“Search for dark matter in proton–proton collisions at 8 TeV with missing transverse momentum and vector boson tagged jets”

-- CMS collaboration --

From arXiv:1607.05764 [hep-ex]

- CMS experiment at the LHC
- $\sqrt{s} = 8\,\mathrm{TeV}$
- Integrated luminosity 19.7 fb^{-1}
- Dark Matter Search

    -- simplified model contact occurs via assumed meditator

DM production via (hypothesis) mediators

$$\mathcal{L}_{\text{vector}} \supset \frac{1}{2} m_{\text{MED}}^2 Z'_\mu Z'^\mu - g_{\text{DM}} Z'_\mu \bar{\chi} \gamma^\mu \chi - g_{\text{SM}} \sum_{\text{q}} Z'_\mu \bar{\text{q}} \gamma^\mu \text{q} - m_{\text{DM}} \bar{\chi} \chi, \tag{1}$$

$$\mathcal{L}_{\text{axial vector}} \supset \frac{1}{2} m_{\text{MED}}^2 \text{A}_\mu \text{A}^\mu - g_{\text{DM}} \text{A}_\mu \bar{\chi} \gamma^\mu \gamma^5 \chi - g_{\text{SM}} \sum_{\text{q}} \text{A}_\mu \bar{\text{q}} \gamma^\mu \gamma^5 \text{q} - m_{\text{DM}} \bar{\chi} \chi, \tag{2}$$

$$\mathcal{L}_{\text{scalar}} \supset -\frac{1}{2} m_{\text{MED}}^2 \text{S}^2 - g_{\text{DM}} \text{S} \bar{\chi} \chi - g_{\text{q}} \sum_{\text{q=b,t}} \frac{m_{\text{q}}}{v} \text{S} \bar{\text{q}} \text{q} - m_{\text{DM}} \bar{\chi} \chi, \tag{3}$$

$$\mathcal{L}_{\text{pseudoscalar}} \supset -\frac{1}{2} m_{\text{MED}}^2 \text{P}^2 - i g_{\text{DM}} \text{P} \bar{\chi} \gamma^5 \chi - i g_{\text{q}} \sum_{\text{q=b,t}} \frac{m_{\text{q}}}{v} \text{P} \bar{\text{q}} \gamma^5 \text{q} - m_{\text{DM}} \bar{\chi} \chi, \tag{4}$$

with $g_{DM} = g_{SM} = 1$, $g_q = 1$

Diagrams of the DM via a scalaer/psedoscalar metiator

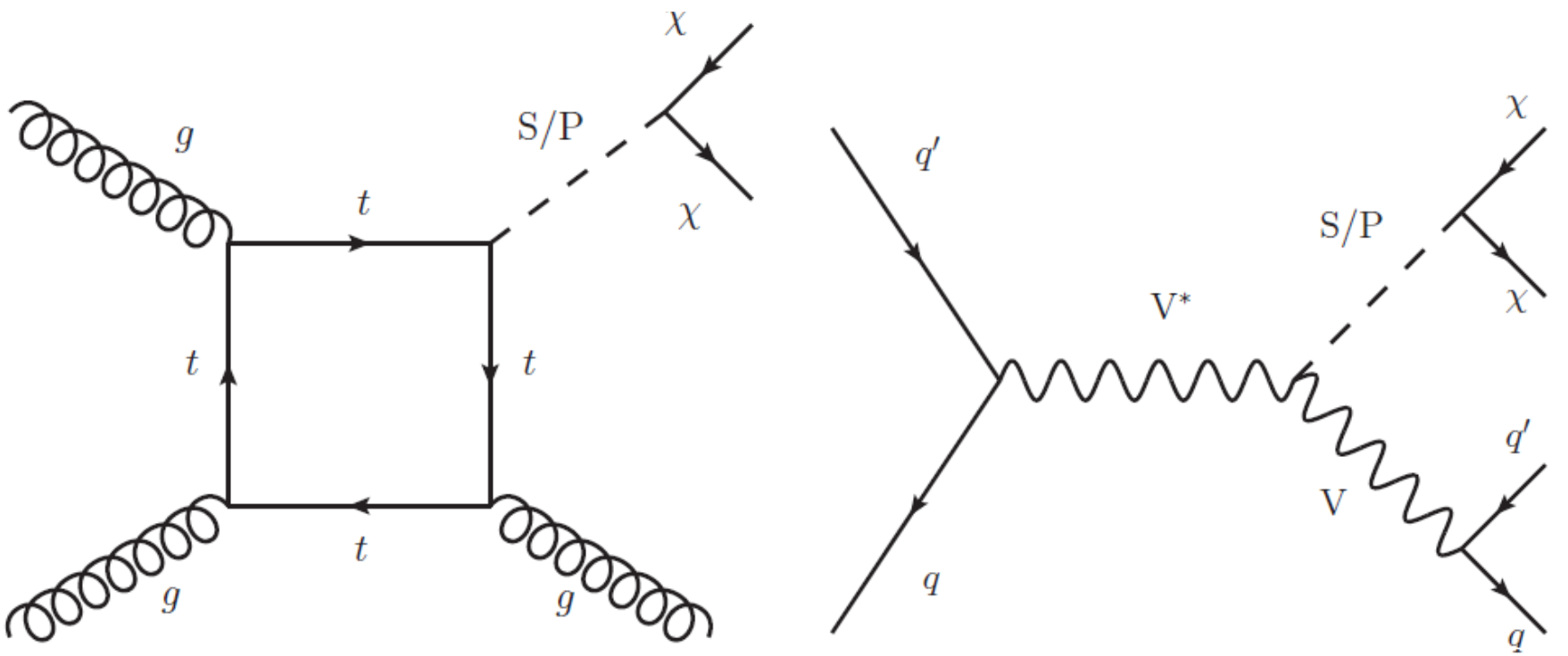

Figure 1: Diagrams for production of DM via a scalar (S) or pseudoscalar (P) mediator in the cases providing monojet (left) and mono-V (right) signatures.

Diagrams of the DM via a vector/axial vector metiator

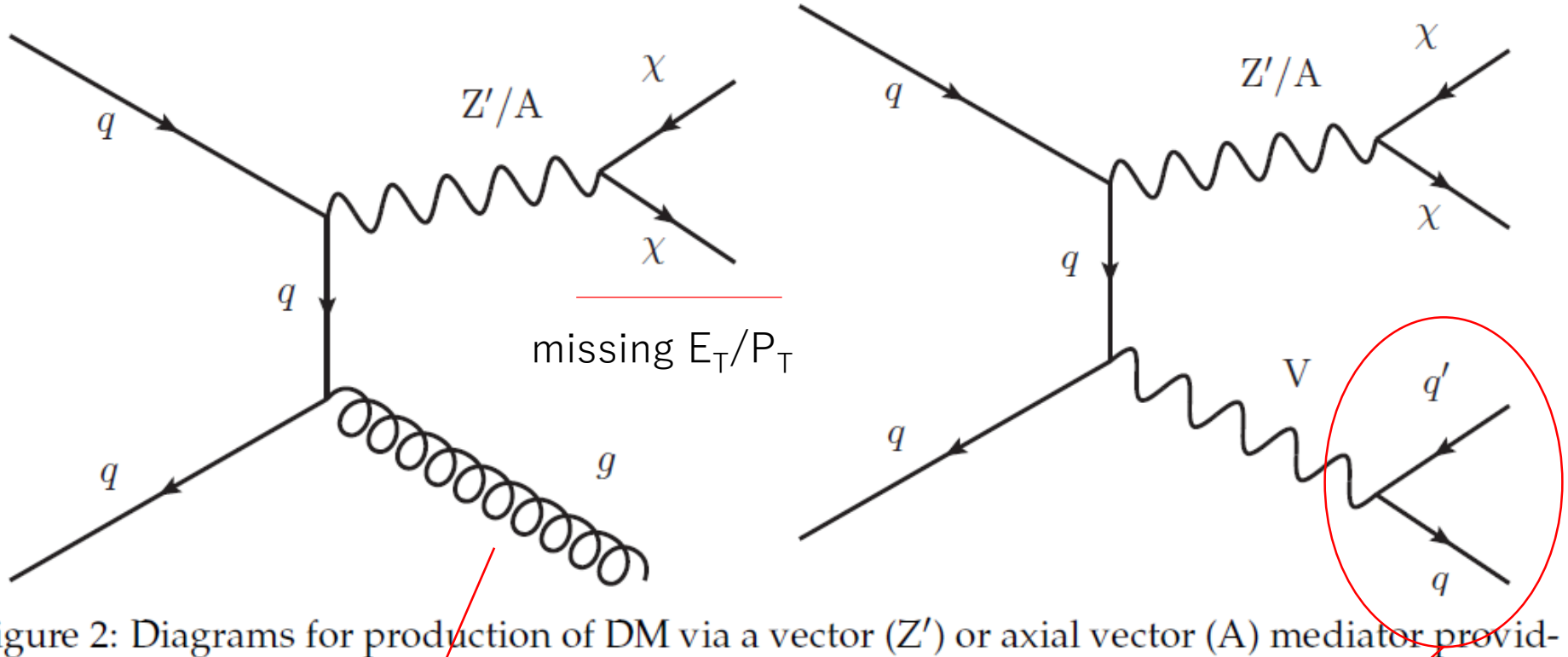

Figure 2: Diagrams for production of DM via a vector (Z′) or axial vector (A) mediator providing monojet (left) and mono-V (right) signatures.

mono jet signal

highly Lorentz-boosted
➔ one cluster
or
resolved into two jets

Background events estimation

signal region

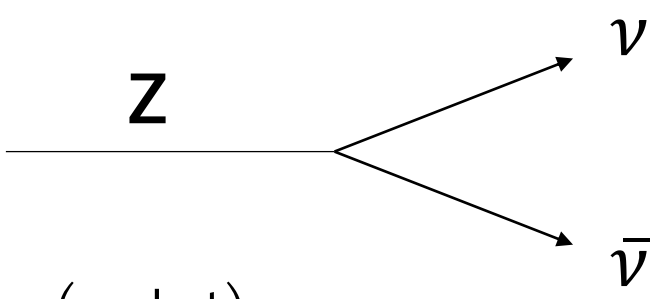

(+ Jet)

control region

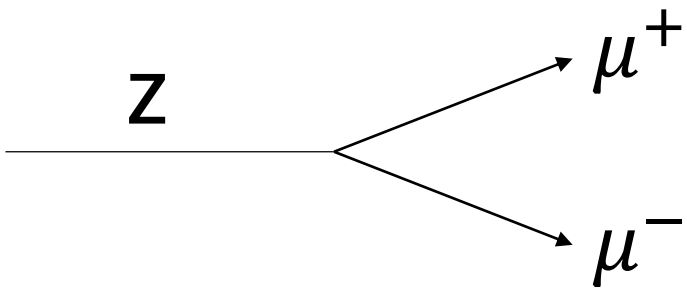

or

high P_T gamma

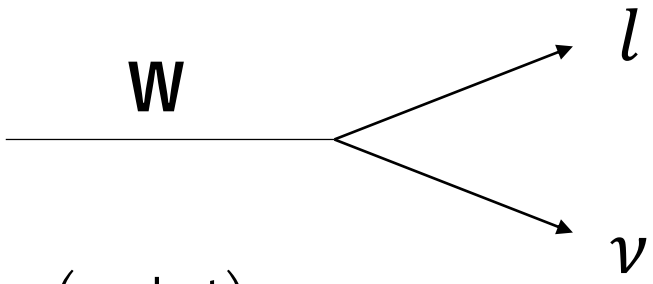

(+ Jet)

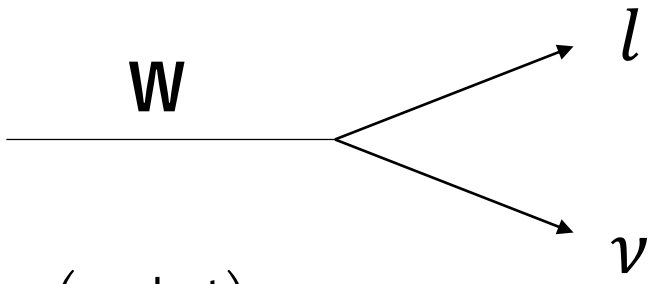

(+ Jet)

Jet Clustering procedure

The extension relative to the k_t and Cambridge/Aachen algorithms lies in our definition of the distance measures:

$$d_{ij} = \min(k_{ti}^{2p}, k_{tj}^{2p}) \frac{\Delta_{ij}^2}{R^2}\,, \tag{1a}$$

$$d_{iB} = k_{ti}^{2p}\,, \tag{1b}$$

where $\Delta_{ij}^2 = (y_i - y_j)^2 + (\phi_i - \phi_j)^2$ and k_{ti}, y_i and ϕ_i are respectively the transverse momentum, rapidity and azimuth of particle i. In addition to the usual radius parameter R, we have added a parameter p to govern the relative power of the energy versus geometrical (Δ_{ij}) scales.

written in reference [27]

in reference [27]

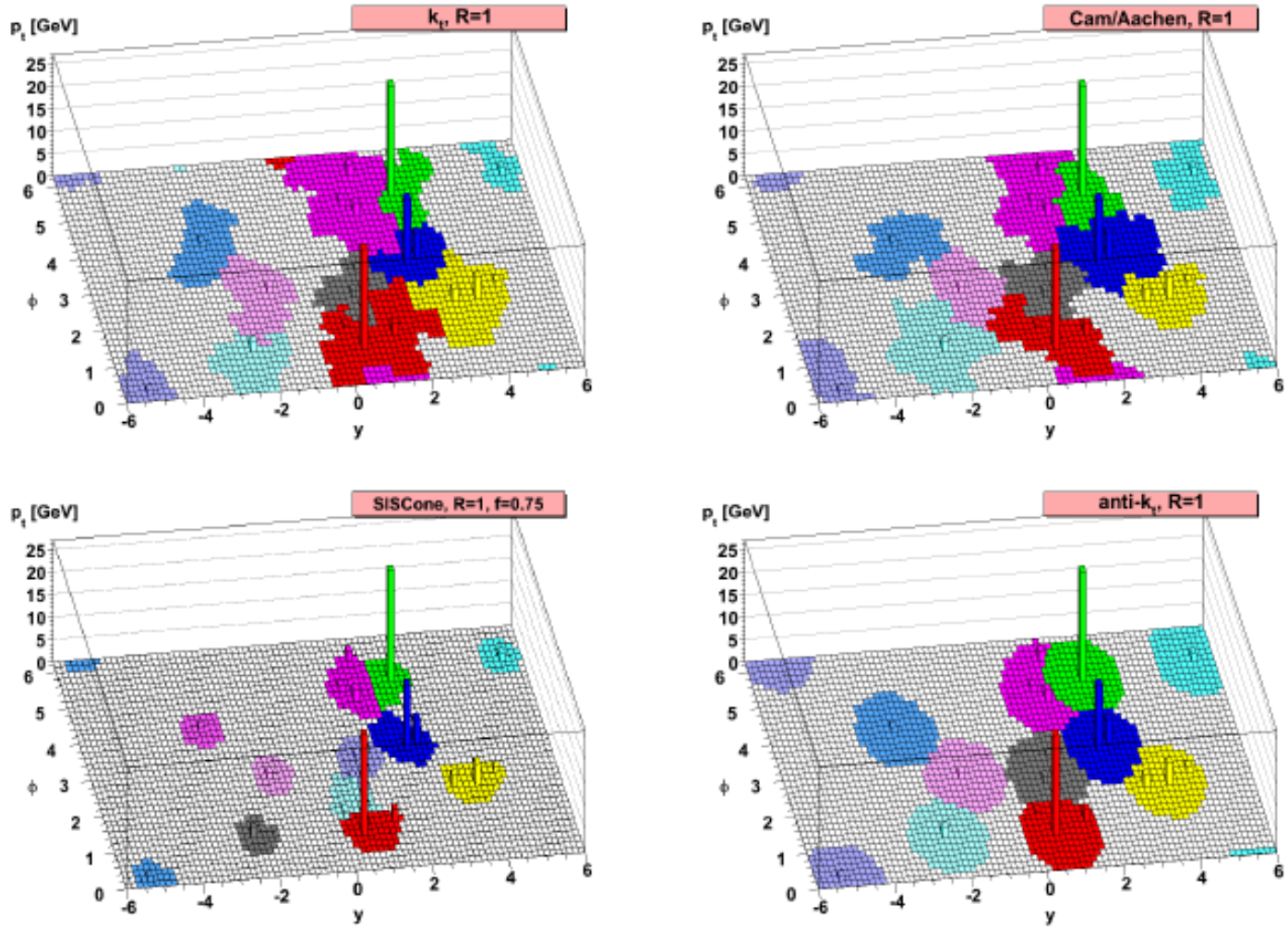

Figure 1: A sample parton-level event (generated with Herwig [8]), together with many random soft "ghosts", clustered with four different jets algorithms, illustrating the "active" catchment areas of the resulting hard jets. For k_t and Cam/Aachen the detailed shapes are in part determined by the specific set of ghosts used, and change when the ghosts are modified.

Jet selection …

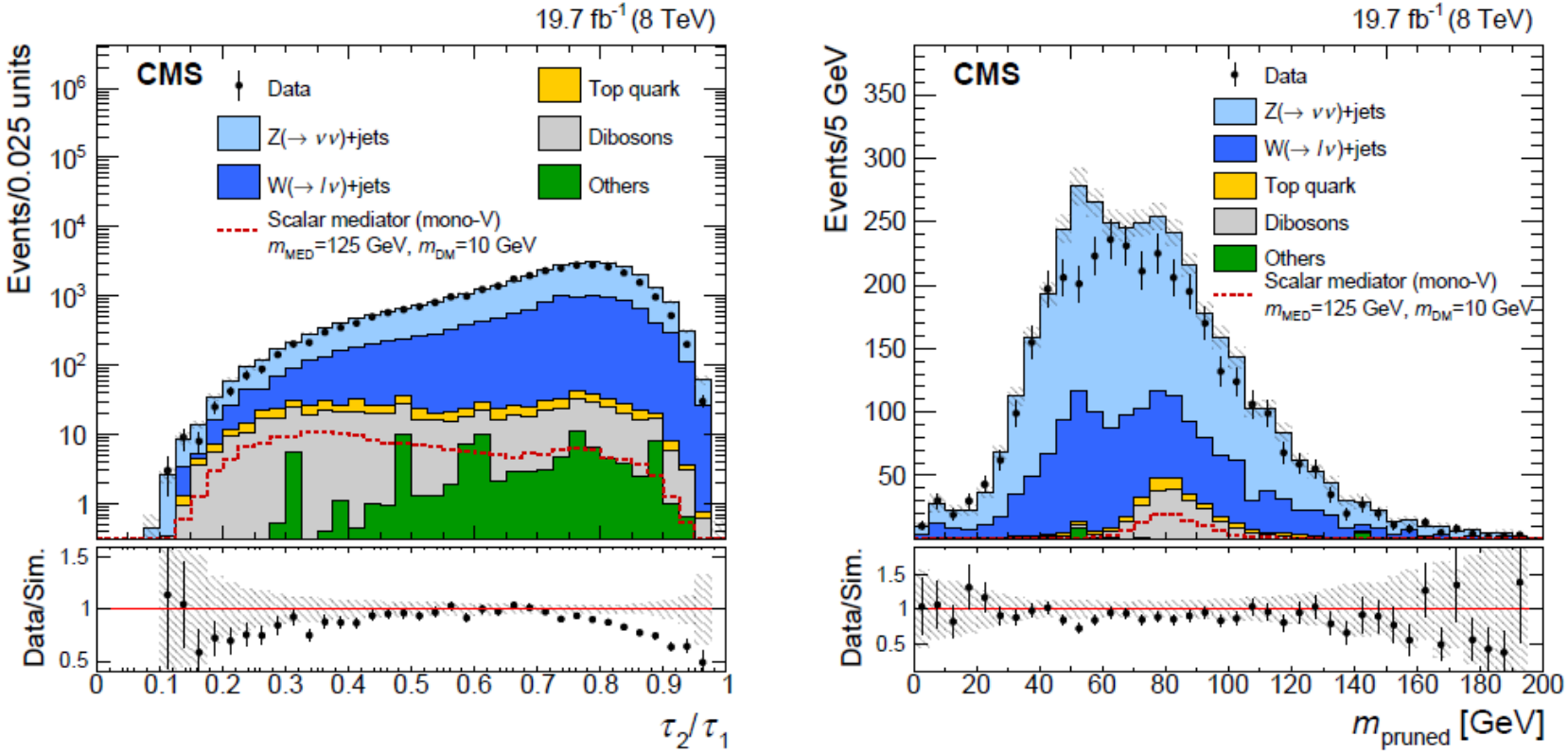

Figure 3: Left: The distribution of τ_2/τ_1 in highly Lorentz-boosted events, before the jet mass selection. Right: The distribution of m_{pruned} for the CA8 jets, before applying the jet mass selection but after the requirement of $\tau_2/\tau_1 < 0.5$ has been applied. The discrepancy between data and simulation is within systematic uncertainties (not shown). The dashed red line shows the expected distribution for scalar-mediated DM production with $m_{\text{MED}} = 125\,\text{GeV}$ and $m_{\text{DM}} = 10\,\text{GeV}$. The shaded bands indicate the statistical uncertainty from the limited number of simulated events.

Reference [65] : tau N

2.1 Introducing N-subjettiness

We start by defining an inclusive jet shape called "N-subjettiness" and denoted by τ_N. First, one reconstructs a candidate W jet using some jet algorithm. Then, one identifies N candidate subjets using a procedure to be specified in Sec. 2.2. With these candidate subjets in hand, τ_N is calculated via

$$\tau_N = \frac{1}{d_0} \sum_k p_{T,k} \min \left\{ \Delta R_{1,k}, \Delta R_{2,k}, \cdots, \Delta R_{N,k} \right\}. \tag{2.1}$$

Here, k runs over the constituent particles in a given jet, $p_{T,k}$ are their transverse momenta, and $\Delta R_{J,k} = \sqrt{(\Delta\eta)^2 + (\Delta\phi)^2}$ is the distance in the rapidity-azimuth plane between a candidate subjet J and a constituent particle k. The normalization factor d_0 is taken as

$$d_0 = \sum_k p_{T,k} R_0, \tag{2.2}$$

Reference [65] : tau N

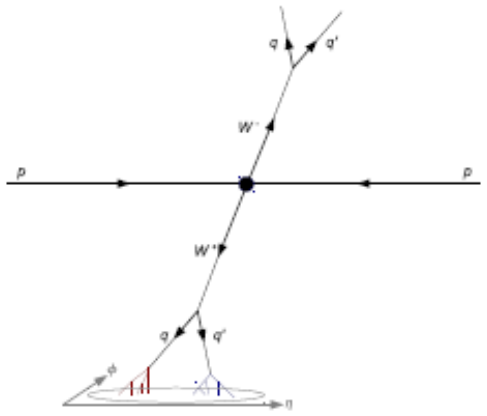

(a)

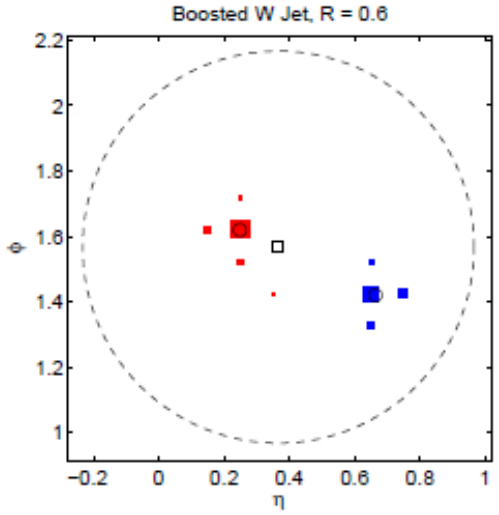

(b)

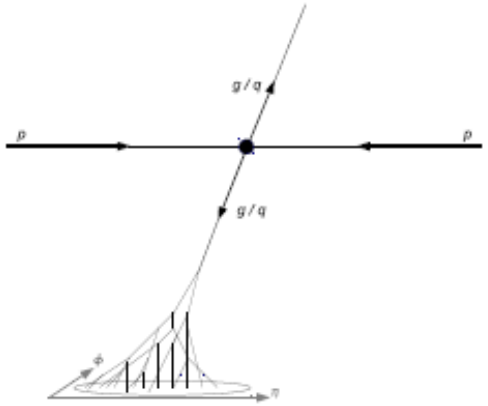

(c)

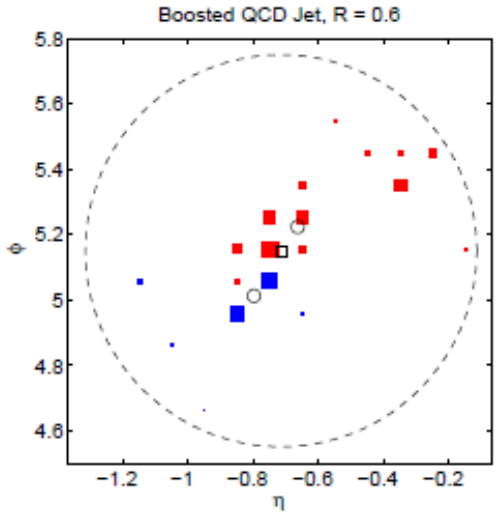

(d)

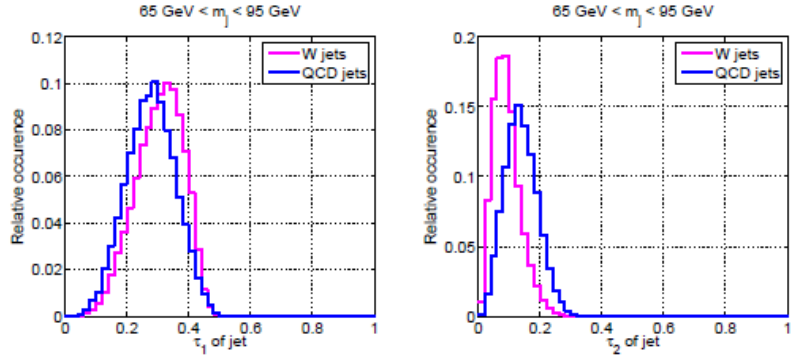

(a) (b)

Figure 2: Distributions of (a) τ_1 and (b) τ_2 for boosted W and QCD jets. For these plots, we impose an invariant mass window of 65 GeV $< m_{\text{jet}} <$ 95 GeV on jets of $R = 0.6$, $p_T > 300$ GeV, and $|\eta| < 1.3$. By themselves, the τ_N do not offer that much discriminating power for boosted objects beyond the invariant mass cut.

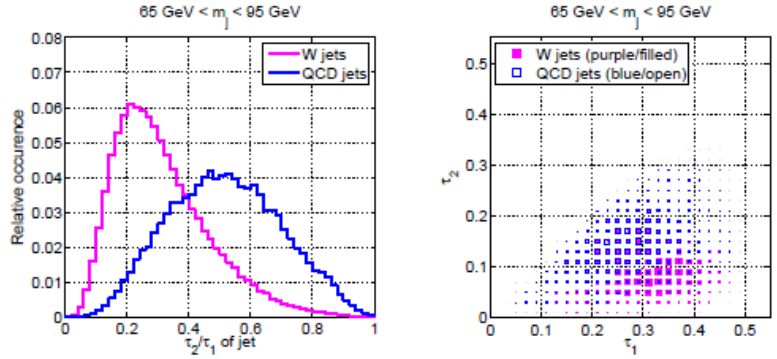

(a) (b)

Figure 3: (a): Distribution of τ_2/τ_1 for boosted W and QCD jets. The selection criteria are the same as in Fig. 2. One sees that the τ_2/τ_1 ratio gives considerable separation between W jets and QCD jets beyond the invariant mass cut. (b): Density plot in the τ_1–τ_2 plane. Marker sizes are proportional to the number of jets in a given bin. In principle, a multivariate cut in the τ_1–τ_2 plane would give further distinguishing power.

Estimation of the SM background events at the control regions (figures) and signal regions (table)

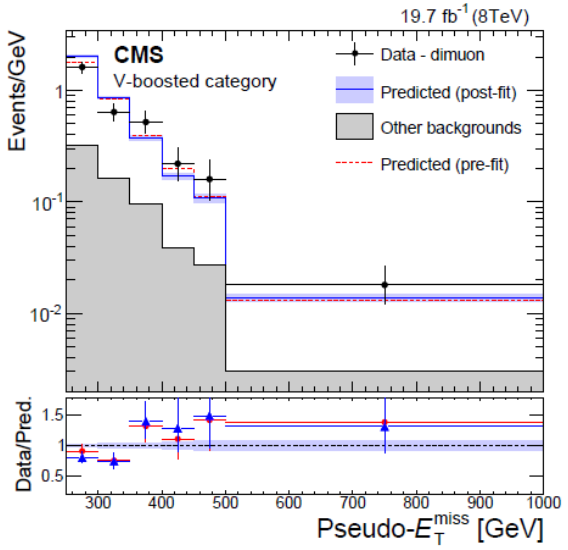

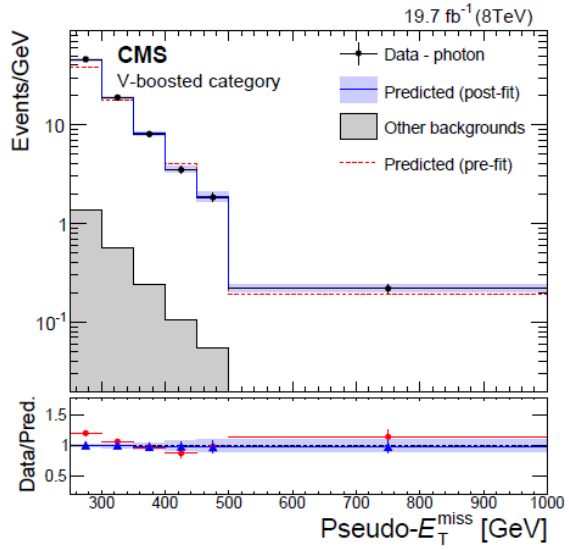

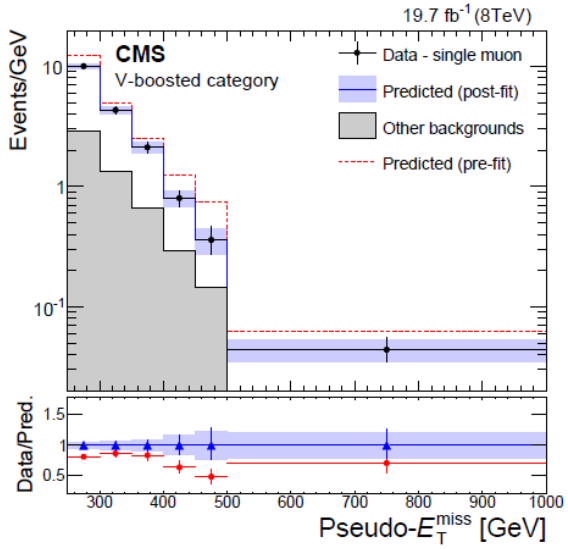

Table 2: Expected yields of the SM processes and their uncertainties per bin for the V-boosted category after the fit to the control regions.

E_T^{miss} (GeV)	Obs.	$Z(\rightarrow \nu\nu)$+jets	$W(\rightarrow \ell\nu)$+jets	Top quark	Dibosons	Other	Total Bkg.
250–300	1073	683±40	279±33	35.4±3.7	103±15	2.5±0.1	1103±63
300–350	453	271±23	114±20	12.7±1.3	46.5±6.9	0.7±0.1	446±34
350–400	160	118±13	38.3±8.7	5.6±1.0	22.2±3.3	0.2±0.1	184±18
400–450	81	49.7±7.3	9.8±3.4	1.5±0.8	11.0±1.8	<0.1	72±29
450–500	30	31.2±6.1	5.0±2.6	0.5±0.1	7.4±1.1	<0.1	44.3±6.6
500–1000	39	39.8±7.8	6.4±3.4	0.2±0.0	7.8±1.1	<0.1	54.3±8.5

Top quarks/ diboson ?? (might be in efficiency of lepton ID ?)

Comparison of E_t^{miss}/leading jet P_T in data and background

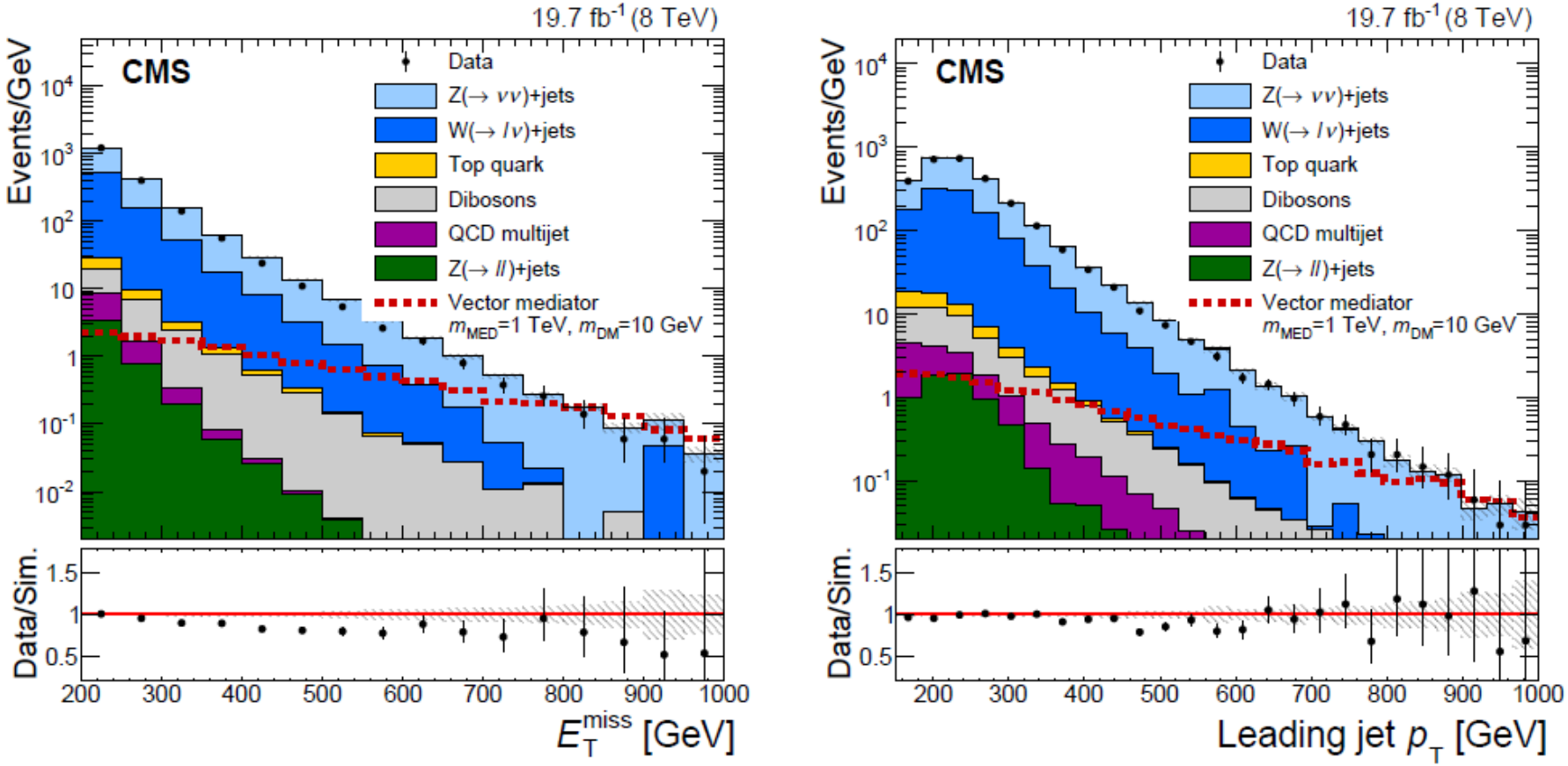

Figure 5: Distributions in E_T^{miss} (left) and leading jet p_T (right) in simulated events and data, resulting from the combined signal selections for the three event categories. The dashed red line shows the expected distribution, assuming vector mediated DM production with m_{MED} = 1 TeV and m_{DM} = 10 GeV. The shaded bands indicate the statistical uncertainty from the limited number of simulated events.

All 3 categories are added.

E_T distributions (w post-fit) Data & Background

Events from the mono jet category is largest among 3 categories …

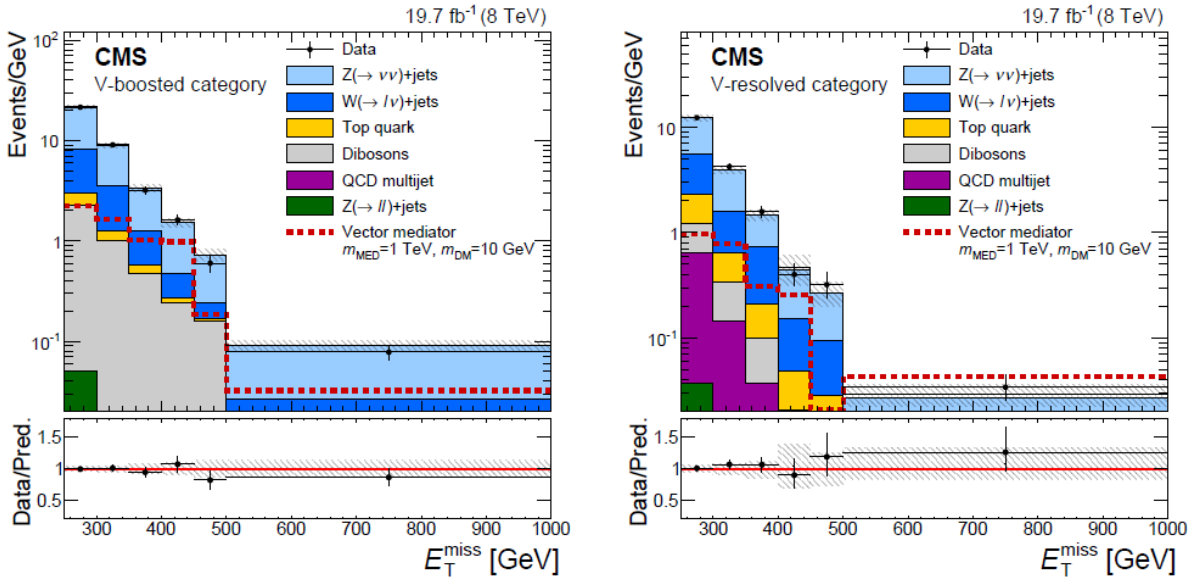

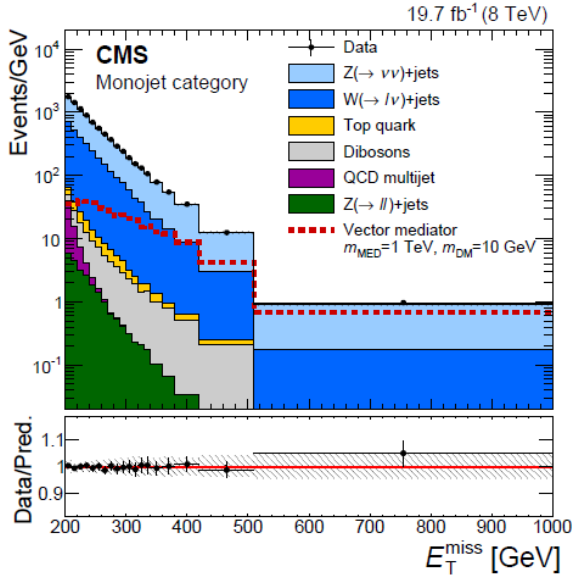

Figure 9: Post-fit distributions in E_T^{miss} expected from SM backgrounds and observed in the signal region. The expected distributions are evaluated after fitting to the observed data simultaneously across the V-boosted (top–left), V-resolved (top–right), and monojet (bottom) categories. The ratio of the data to the post-fit background prediction is shown in the lower panels. The shaded bands indicate the post-fit uncertainty in the background, assuming no signal. The horizontal bars on the data points indicate the width of the bin that is centred at that point. The expected distribution for a signal assuming vector mediated DM production is shown for $m_{MED} = 1\,TeV$ and $m_{DM} = 10\,GeV$.

90% C.L. exclusion limit (contours) on the M_{MED} - M_{DM}

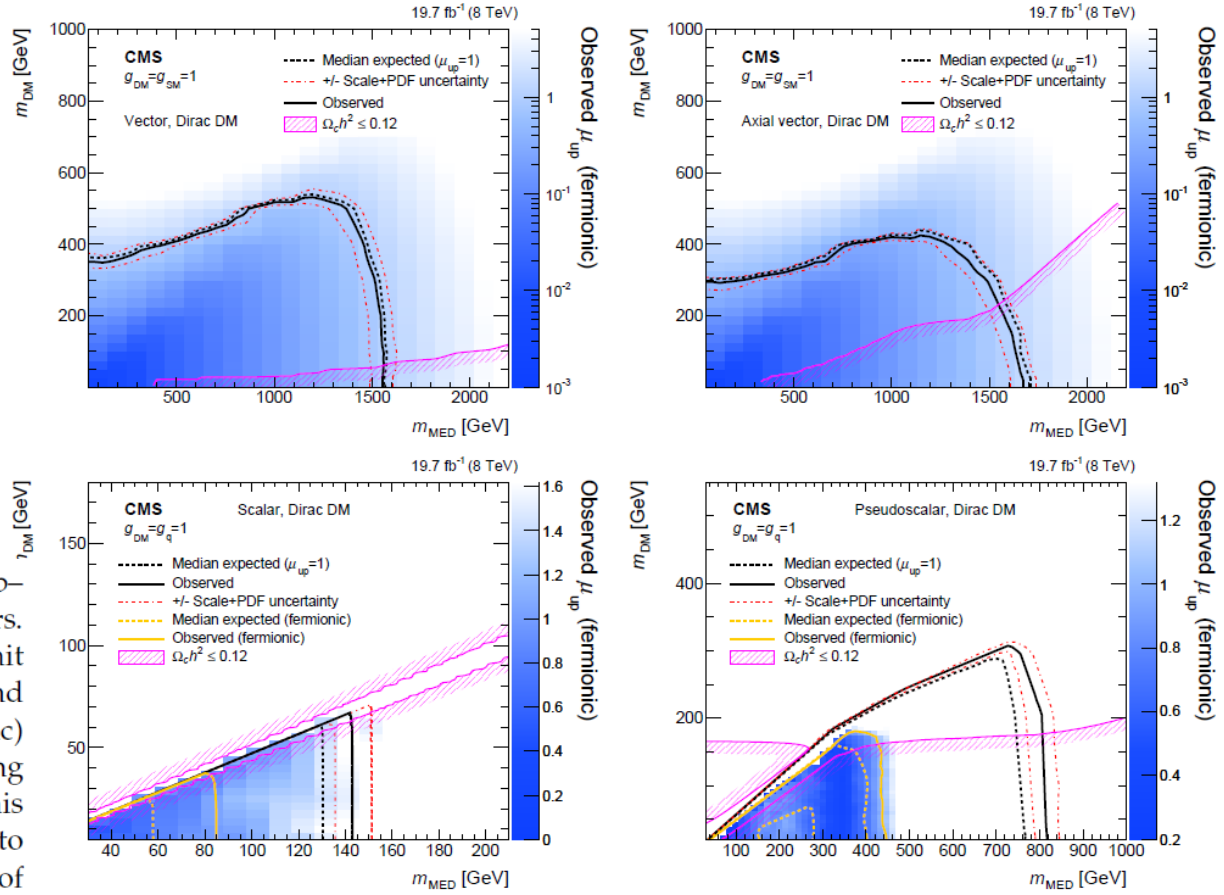

Figure 10: The 90% CL exclusion contours in the $m_{\mathrm{MED}} - m_{\mathrm{DM}}$ plane assuming vector (top–left), axial vector (top–right), scalar (bottom–left), and pseudoscalar (bottom–right) mediators. The scale shown on the right hand axis shows the expected 90% CL exclusion upper limit on the signal strength, assuming the mediator only couples to fermions. For the scalar and pseudoscalar mediators, the exclusion contour assuming coupling only to fermions (fermionic) is also shown. The white region shows model points that were not tested when assuming coupling only to fermions and are not expected to be excluded by this analysis under this assumption. The red dot-dashed lines indicate the variation in the exclusion contours due to modifying the renormalization and factorization scales by a factor of two in the generation of the signal. In all cases, the excluded region is to the bottom–left of the contours, except for the relic density, which shows the regions for which $\Omega_c h^2 = 0.12$, as indicated by the shading. In all of the models, the mediator width is determined using the minimum width assumption.

From reference [88]

cold dark matter density

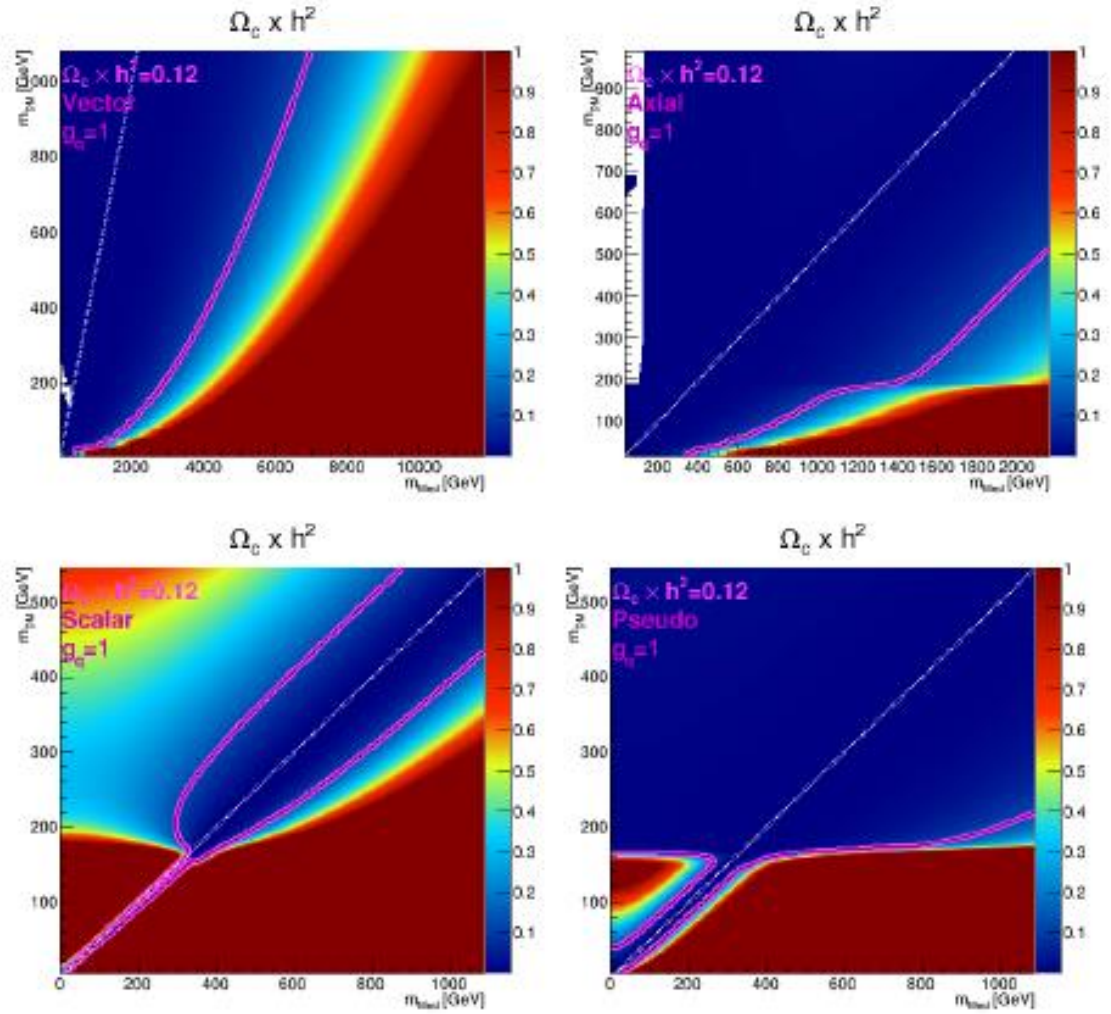

Figure 1. The predicted DM relic density for the vector, axial-vector, scalar, and pseudo-scalar mediators for coupling $g_q = g_{SM} = g_{DM} = 1$. The white dashed line corresponds to the region where $M_{\mathrm{Med}} \sim 2 \times M_{DM}$. The pink curve denotes the masses for which the predicted relic DM coincides with the observed $\Omega_c \times h^2 = 0.12$ [1].

90% C.L. exclusion limit (contours) on the M_{DM} – cross_section histos

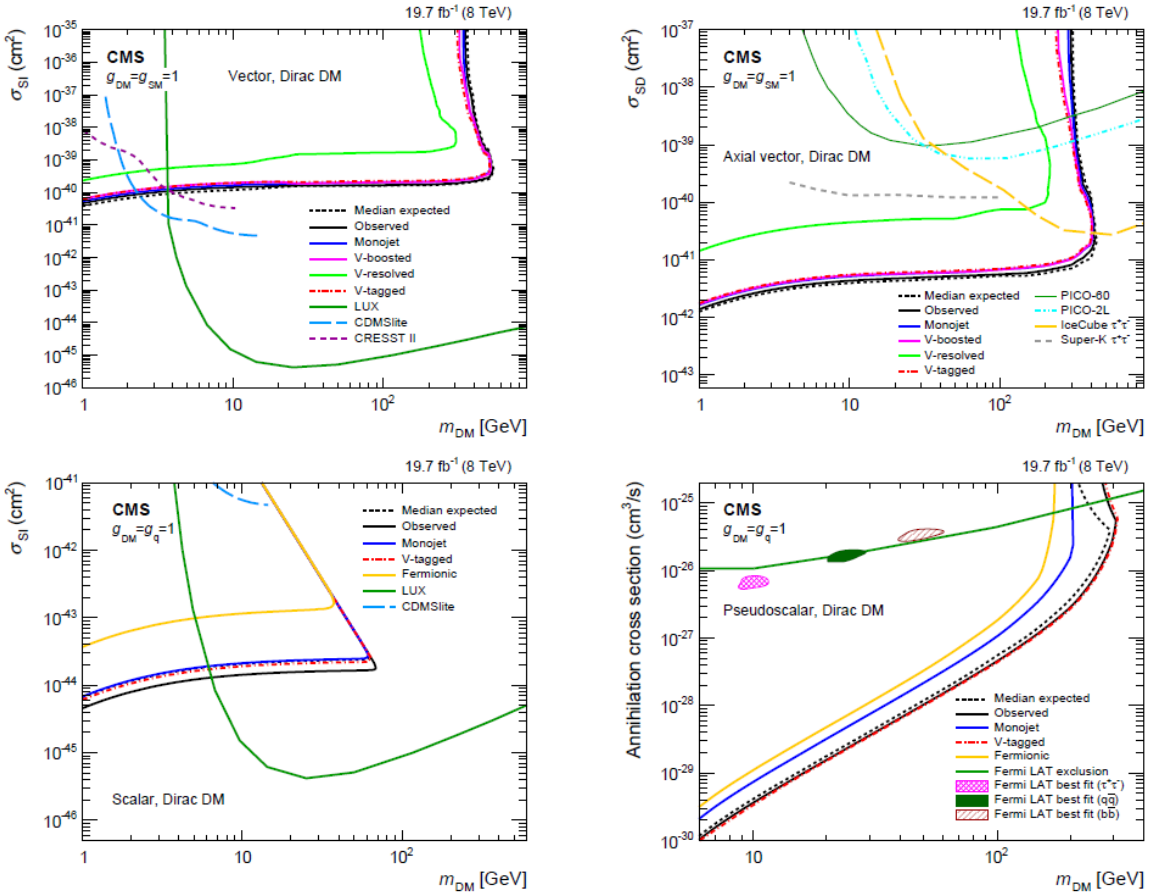

Figure 11: The 90% CL exclusion contours in the $m_{DM} - \sigma_{SI}$ or $m_{DM} - \sigma_{SD}$ plane assuming vector (top–left), axial vector (top–right), scalar (bottom–left) mediators. Also shown is the 90% CL exclusion in DM annihilation cross section as a function of m_{DM} for a pseudoscalar mediator (bottom–right). For the scalar and pseudoscalar mediators, the exclusion contours assuming the mediator only couples to fermions (fermionic) is also shown. The excluded region in all plots is to the top–left of the contours for the results from this analysis while the DD experiment and Fermi LAT excluded regions are above the lines shown. In the vector and axial vector models, limits are shown independently for monojet, V-boosted, and V-resolved categories. The red dot-dashed line shows the partial combination of the V-tagged categories for which the V-boosted category provides the dominant contribution. In all of the mediator models, a minimum mediator width is assumed. For the pseudoscalar mediator, 68% CL preferred regions, obtained using data from Fermi LAT, for DM annihilation to light-quarks ($q\bar{q}$), $\tau^+\tau^-$, and $b\bar{b}$ are given by the solid green, hatched pink, and shaded brown coloured regions, respectively.

Summary

“ This search is the first at CMS to use jet substructure techniques to identify hadronically decaying vector bosons in both Lorentz-boosted and resolved scenarios.”

“ No significant deviation is observed”

“ The search excludes DM production via vector or axial vector mediation with mediator masses up to 1.5TeV, within the simplified model assumptions”

“ For scalar and pseduscalar mediated DM production, this analysis excludes mediator masses up to 80 and 400 GeV, respectively”

-- from the Summary section